06

Improvement physical and mechanical properties of Ti-6Al-4V alloy processed by selective laser melting

© M.Yu. Gryaznov, S.V. Shotin, V.N. Chuvil'deev, A.V. Semenycheva, A.N. Sysoev, A.V. Piskunov

Lobachevsky University of Nizhny Novgorod,
603022 Nizhny Novgorod, Russia
e-mail: semenycheva@nifti.unn.ru

Received September 7, 2023
Revised November 14, 2023
Accepted December 14, 2023

The physical and mechanical properties of Ti-6Al-4V titanium alloy processed by selective laser melting were studied. It is shown that the strength characteristics under optimal fusion conditions (strength limit 1300 MPa and conditional yield strength 1250 MPa) are 30% higher than the standard values for this alloy made using traditional technologies (rolling, forging). The reason for the increase in the strength characteristics of the Ti-6Al-4V alloy is the presence of a finely dispersed martensitic $\alpha + \beta$ structure formed due to high crystallization rates realized during selective laser melting. At the same time, the optimization of scanning tactics allows to achieve elongation to failure of 11% by reducing porosity and the level of internal stresses.

Keywords: titanium alloy Ti-6Al-4V, additive technologies, selective laser melting, density, strength, plasticity, microstructure, implants for surgery.

DOI: 10.21883/0000000000

Introduction

The alloy of the Ti-6Al-4V system is an $\alpha + \beta$ titanium alloy with increased specific strength, high incorrodibility and sufficient bioinertness [1,2]. This alloy has found wide application in the aerospace and chemical industries, as well as biomedicine [2–5]. High specific strength and bioinertness make it possible to use the Ti-6Al-4V alloy as a material for the manufacture of endoprostheses and implants [1,5,6]. At the same time, the manufacturing of products from this alloy is a difficult problem due to its low thermal conductivity, susceptibility to strain hardening and active chemical reaction with oxygen during heat treatment [7,8]. Traditional manufacturing of Ti-6Al-4V alloy products, based on casting, forging and rolling followed by machining to obtain final shapes, has low materials utilization rate and in general is distinguished by high manufacturing costs [3,5].

In recent years, numerous attempts have been made to develop additive manufacturing technology for titanium alloy products as an alternative manufacturing technology. In particular, selective laser melting (SLM) is a promising technology due to its high production flexibility, the ability to obtain final products that do not require machining, a short production cycle and minimal material loss compared to traditional types of machining process [9,10]. In the future, SLM may become a key technology for the manufacture of medical implants with unique osteo-inductive properties and complex geometry that cannot be manufactured by other methods [11,12] In particular, SLM makes it possible to produce structured porous structures (scaffolds, gyroids), which improve the fixation and osseointegration of implants and endoprostheses [11,13,14].

Currently, numerous works have been carried out to optimize the process of manufacturing products from the Ti-6Al-4V alloy (Grade 5, Grade 23, etc.) using additive technologies [1,5,15]. At the same time, a number of problems remain unresolved related to the presence of internal defects, residual stresses and a decrease in plastic properties compared to similar wrought alloys, which prevents the wide application of additive technologies for the manufacturing of medical products. In order to solve these problems, many researchers have studied the influence of SLM parameters on the microstructure and mechanical behavior of the Ti-6Al-4V alloy. In particular, it has been established that the Ti-6Al-4V SLM alloy has a wide range of tensile strength values from 900 to 1300 MPa and elongation to failure from 1 to 10% depending on the SLM process parameters [16,17,19]. One of the main reasons for such a range in the values of mechanical characteristics are macrostructural defects (pores, cracks and unmelted powder particles), which arise during rapid crystallization and a high temperature gradient during the SLM process. In this regard, current paper aimed to optimizing SLM modes to obtain a Ti-6Al-4V alloy with characteristics that meet the requirements for titanium alloys for medical applications [20]. To resolve this problem, a systematic study of the influence of SLM parameters, including laser power and scanning speed, as well as scanning tactics on the physical and mechanical properties of the Ti-6Al-4V alloy manufactured by the SLM method, was carried out.

1. Methodology for studying properties and structure

Studies of the granulometric composition of the powder were carried out using a SALD-2300 Shimadzu Laser Diffraction Particle Size Analyzer by dry screening. The density of samples produced by the SLM method in the form of cubes with dimensions $10 \times 10 \times 10$ mm, was measured by hydrostatic weighing on Sartorius CPA225D analytical balance and is presented as a percentage of the theoretical density of the Ti-6Al-4V alloy Grade 5, amounting to 4.43 g/cm^3 [21]. Tensile tests were carried out using Tinius Olsen H25K-S Testing Machine at room temperature for cylindrical samples with a working area with diameter and length equal to 3 and 15 mm, respectively. The tests were carried out with a constant deformation velocity of 0.01 mm/s. The samples for mechanical testing were built on the platform of the SLM machine in a vertical orientation (the longitudinal axis of the samples was parallel to the axis of the laser beam). Structural studies were carried out using Jeol JSM 6490 and Tescan Vega 2 scanning electron microscopes. For metallographic studies, cubic samples with dimensions $10 \times 10 \times 10$ mm were cutting by electrical discharge machining along the central plane (XY-plane is laser beam scanning during SLM), then the surface was mechanically was polished using diamond pastes and subjected to electrochemical etching.

2. Methodology for achievement of samples

The subject of research are samples of titanium alloy Ti-6Al-4V (hereinafter referred to as Ti-6Al-4V SLM alloy), manufactured using SLM technology on a modernized Equipment MTT (Realizer SLM 100) from powder produced by the company „TLS Technik". The powder particles have a spherical shape with an average size of 35 μm and a particle size distribution from 20 to 70 μm. Chemical composition of the powder according to the manufacturer's certificate (wt.%): Al — 6.3%; V — 4.5%; Fe — 0.2; O — 0.15; C — 0.05; N — 0.03; H — 0.005; Ti — base. Powder flowability measurements were carried out in accordance with ISO 4490:2018. The flowability of the powder after processing in a vacuum oven at a temperature of 210° for 3 h was about 20 s, which is sufficient for uninterrupted supply of powder and the formation of a homogeneous powder layer on the platform during the SLM process.

45 series of samples were produced by SLM with different modes: laser power P varied from 60 to 100 W (with a change step of 10 W), the scanning speed V — from 30 to 600 mm/s (9 scanning speed values were used: 30, 50, 100, 150, 200, 300, 400, 500 and 600 mm/s). The other SLM parameters remained constant during the construction of all samples: powder layer thickness $d = 70\,\mu$m, hatch spacing $s = 120\,\mu$m. As a basic scanning tactic, we chose to rotate the hatching by 90° in each subsequent layer. This tactic was used to optimize the strength properties of the material. For optimizing plasticity, samples were processed using the „chessboard" scanning tactic (the cell size was varied) and the rotation of hatching (angle of rotation was varied). The platform with a diameter of 100 mm was made of titanium alloy VT6 (analogue of the Ti-6Al-4V alloy), the temperature of the platform was maintained constant and amounted to 200°C. The samples were cut from the platform by electrical discharge machining. All manipulations with the powder (vibration sieving, drying in a heat chamber, etc.) and the SLM process were carried out in high-purity argon (99.998 wt.%). Diagrams of physical and mechanical properties in coordinates „laser power — scanning speed" in Fig. 1 – were constructed in the MATLAB R2022 package by cubic spline approximation of experimental points, which are matrices 5×9 of parameter values P and V.

To quantitatively characterize SLM modes, the concept of volumetric energy density [22–25] is used, which determines the amount of energy received per unit volume of material during the SLM process. As a rule, this value can be estimated using the expression $E = P/Vds$ [24,25].

3. Results of experimental studies

Studies have been carried out of the influence of SLM process parameters on the physical and mechanical characteristics of the Ti-6Al-4V alloy. The experimental values of the mechanical characteristics indicated in the diagrams were obtained by averaging the results obtained on two samples. Fig. 1 shows a diagram of the dependence of the tensile strength on the laser power and scanning speed. As can be seen from the figure, the maximum value of the tensile strength of 1300 MPa is observed at the following SLM parameters: laser power 90 ± 10 W and scanning speed 100 ± 25 mm/s. The minimum tensile strength value of 800 MPa was obtained using laser power 65 ± 5 W and scanning speed 550 ± 50 mm/s. Fig. 2 shows a diagram of the dependence of the yield stress on the laser power and scanning speed. The maximum yield strength value of

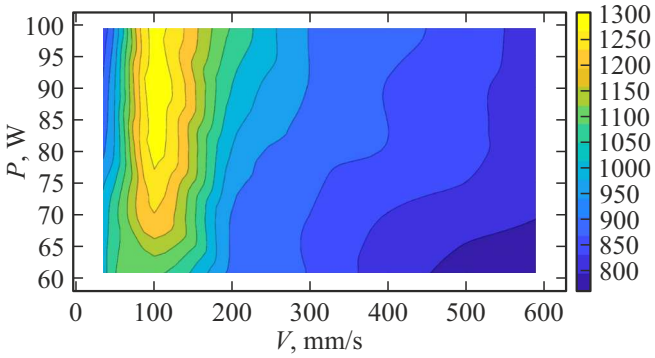

Figure 1. Dependence of the tensile strength of Ti-6Al-4V SLM alloy on laser power and scanning speed

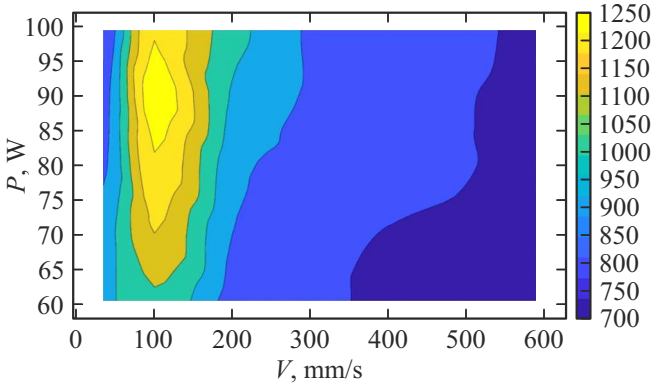

Figure 2. Dependence of the tensile strength of Ti-6Al-4V SLM alloy on laser power and scanning speed

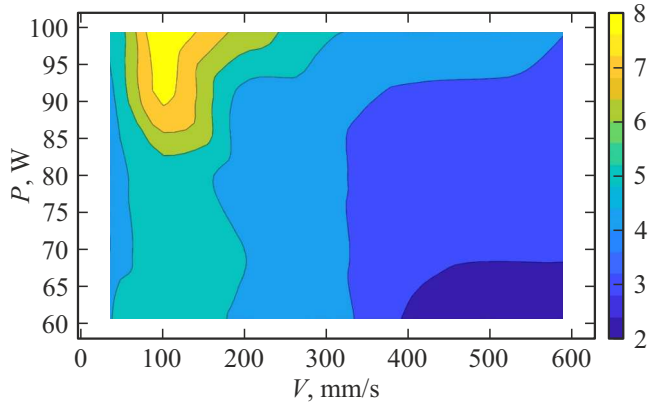

Figure 3. Dependence of elongation to failure of Ti-6Al-4V SLM alloy on laser power and scanning speed.

90 ± 5 W was obtained using laser power 90 ± 5 W and scanning speed 100 ± 10 mm/s, and the minimum value of 700 MPa — using laser power 60 ± 5 W and scanning speed 500 ± 100 mm/s. The maximum value of elongation to failure of 8.0% was obtained in the range of SLM parameters: laser power 90 ± 10 W and scanning speed 100 ± 10 mm/s (Fig. 3), the minimum value of 2.0% was obtained by using laser power 65 ± 5 W and scanning speed 500 ± 100 mm/s.

A study was carried out of the influence of SLM parameters on the density of the Ti-6Al-4V alloy. Fig, 4 shows a diagram of the dependence of the relative density ρ on the laser power and scanning speed. The figure shows that the maximum values of the relative density $99.4 \pm 0.1\%$ were obtained with the following SLM parameters: laser power 95 ± 5 W and scanning speed 100 ± 50 mm/s. The minimum relative density value of 82% was obtained by using laser power 65 ± 5 W and a scanning speed of more than 550 mm/s.

The structure of SLM samples of the Ti-6Al-4V alloy was studied using by optical and scanning electron microscopy. Typical image of the microstructure of an SLM alloy is shown in Fig. 5. During the SLM process, a martensitic finely dispersed $\alpha + \beta$-microstructure is formed, typical of the Ti-6Al-4V [22,26] SLM alloy. It is shown that the characteristic dimensions of martensite plates (needles) are $2 \times 30\,\mu$m, the average size of a martensite packet is $50\,\mu$m. The quantitative characteristics of the martensitic structure weakly depend on the SLM parameters; the main difference in the microstructure is the presence of defects (pores and cracks) observed in the structure of alloy samples obtained in non-optimal SLM modes. As is known, defects arising during SLM have different formation mechanisms, depending on the technological parameters [22,27]. In this work, three types of macroscopic defects are observed in the SLM material. Firstly, large volumetric pores in the plane of laser beam scanning, i.e. pores, the occurrence of which is associated with low values of volumetric energy density (5 ± 15 J/mm^3), which do not ensure complete melting of powder particles (Fig. 6, *a*). In Fig. 1–4, a similar type of defect corresponds to a region in the range of parameter values P 60–70 W and V 500–600 mm/s. The second type of defects, i.e. small pores (with a diameter of less than $5\,\mu$m), the occurrence of which is associated with a high volumetric energy density (more than 200 J/mm^3), leading to overheating and splashing of

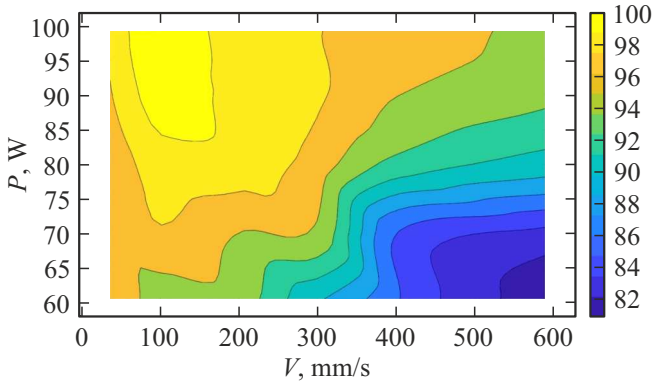

Figure 4. Dependence of the relative density of the Ti-6Al-4V SLM alloy on the laser power and scanning speed.

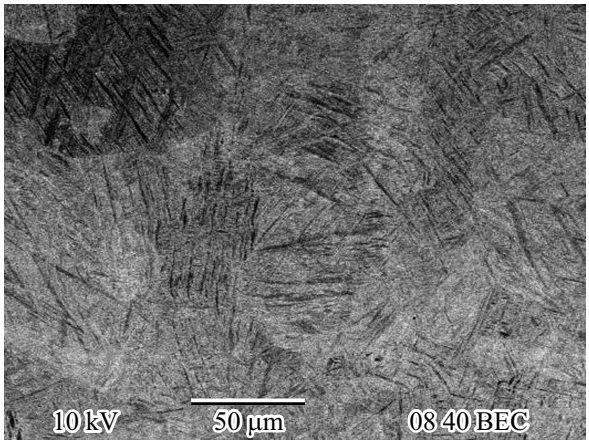

Figure 5. Typical microstructure of Ti-6Al-4V alloy samples obtained using by selective laser melting

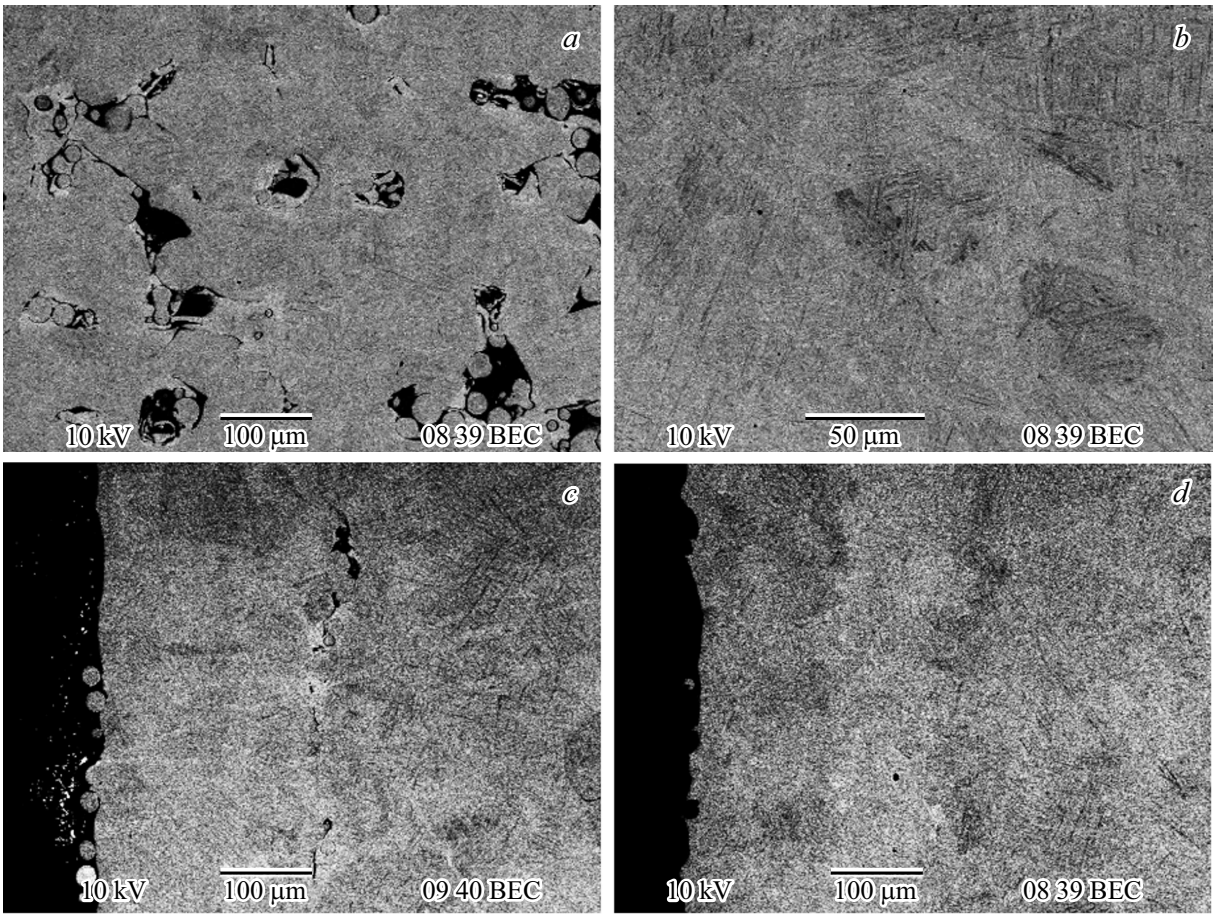

Figure 6. Defects in the structure of the Ti-6Al-4V SLM alloy: pores, the occurrence of which is associated with low (a) and high (b) volumetric energy density, defects at the boundary between contours and hatching without optimization scanning tactics (c) and defect-free structure at the boundary between contours and hatching after optimizing the scanning tactics (d).

the melt pool (Fig. 6, b) [27,28]. In Fig. 1−4, a similar type of defect corresponds to a region in the range of parameter values P 90−100 W and V 25−50 mm/s. The third type is microcracks that appear in the material at the boundary between areas with different scanning tactics, as a rule, at the boundary between the contours and the main hatching of the cross-sectional area (Fig. 6, c). The volume fraction of such defects in the material does not exceed 0.3%, and they can significantly affect its mechanical properties. In Fig. 1−4 a similar type of defects is observed in a wide range of SLM parameters, including in the set of optimal values P 95 ± 5 W and V 125 ± 25 mm/s.

Analysis of the experimental results showed that the maximum values of the yield stress and tensile strength (1250 and 1300 MPa, respectively) were obtained on samples with a maximum density of 99.4%, which is observed by using laser power 95 ± 5 W and scanning speed 125 ± 25 mm/s. The high strength characteristics obtained in this work can be explained by the presence of finely dispersed $\alpha + \beta$ martensite, the appearance of which is associated with a high crystallization rate ($10^5 - 10^7$ K/s) during the SLM process. The value of relative elongation to failure in the optimal mode does not exceed 8.0%. According to GOST R ISO 5832-3-2020, which defines the basic requirements for the physical and mechanical characteristics of titanium alloy Ti-6Al-4V, the tensile strength of the material must be at least 860 MPa, while the elongation after break must be at least 10% [20]. Thus, the tensile strength of the SLM alloy without heat treatment is 30% higher than the required value of the tensile strength, while the obtained plastic characteristics of the SLM alloy do not meet the requirements of the standard. Similar results are observed in many experimental works on studying the properties of the Ti-6Al-4V SLM alloy (see table). An increase in the ductility of Ti-6Al-4V samples produced by SLM can be achieved by hot isostatic pressing (HIP) or heat treatment, which usually leads to a decrease in the strength characteristics of the material [17,26,30–32]. Finished products with complex geometries, including medical products with scaffolds used to create endoprostheses, can lose the accuracy of their geometry during HIP, while heat treatment of products containing thin walls, lattices, etc. can lead to the formation heterogeneous microstructure and, as a consequence, to anisotropy of the mechanical characteristics of the material.

Comparison of mechanical properties of Ti-6Al-4V alloy produced using different technologies

Condition/technology	Tensile strength, MPa	Yield strength, MPa	Elongation to failure, %	Reference
SLM	1241	1065	6	[17]
SLM + annealing	945	869	18	[17]
SLM + HIP	941	839	19	[17]
SLM	1114	1058	3	[18]
SLM	1361	1209	2.8	[31]
SLM + annealing	1132	1067	7.6	[31]
SLM	1334	1110	6.35	[33]
SLM	1151	946	4.4	[34]
SLM	1235	1105	11.2	[32]
SLM + annealing	975	893	26.4	[32]
SLM	1041	962	15	[35]
SLM+ annealing	910	860	15	[35]
SLM	1300	1250	8	This work
Forging	1008	962	19	[18]
Forging	932	846	15	[34]
Casting	980	880	13.5	[36]
Rolling	$\geq$ 890	$\geq$ 795	$\geq$ 10	[20]
Casting	$\geq$ 860	$\geq$ 758	$\geq$ 8	[37]

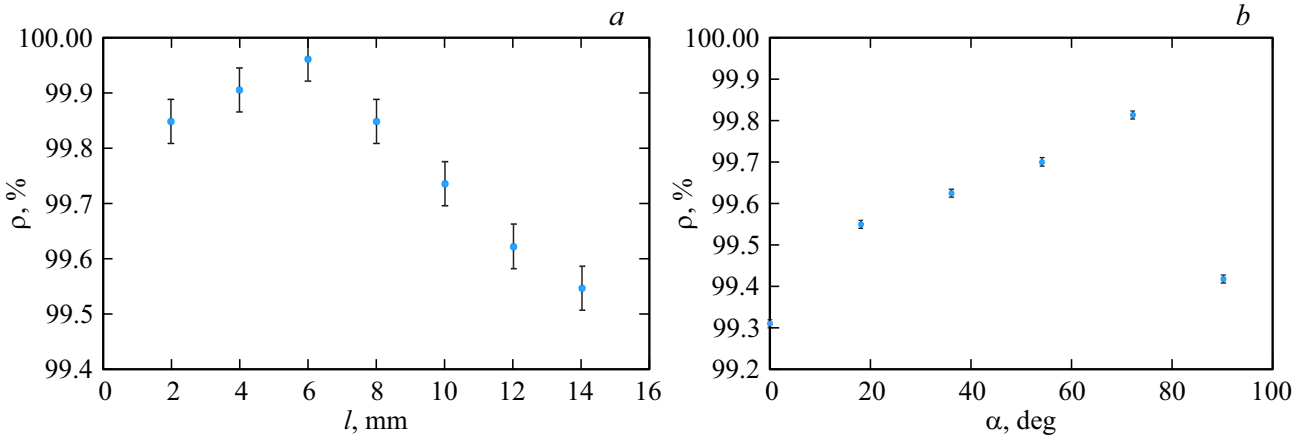

Figure 7. Dependence of relative density ρ of Ti-6Al-4V SLM alloy on (a) cell side length l (scanning tactics „chessboard"); (b) hatch rotation angle relative to the previous layer α.

Another approach to increasing plasticity is to optimize scanning tactics to reduce porosity and internal stress levels. As is known, SLM is a multi-parameter technological process. An important role played scanning tactics, which is a set of parameters that determine the set of trajectories along which the laser beam moves and the order in which they pass. This work discusses ways to increase density and plasticity by reducing the number of internal defects by optimizing scanning tactics. One of the most common scanning tactics is „chessboard". This is a tactic in which the entire cross-section of the sample is divided into squares i.e. cells, each of which is hatched separately [27,38]. In this case, the variable parameters are the cell size, the order of cell hatching, the angle

of inclination of the hatching inside each cell relative to the boundaries or the previous layer. To study the effect of scanning tactics on the relative density of the alloy, 7 series of samples with dimensions $30 \times 30 \times 10$ mm and different cell side lengths l were processed: 2, 4, 6, 8, 10, 12, and 14 mm. The results of the relative density study are presented in Fig. 7, *a*. As can be seen from the figure, the relative density at the optimal cell side length 6 mm was 99.95%, while increasing the cell side length to 14 mm leads to a decrease in the relative density to 99.55%. This effect is usually associated with an increase in the temperature gradient inside the cell with large linear dimensions „square" [39].

It is known that changing the hatch rotation angle relative to the previous layer in the range $0-90^\circ$ makes it possible to reduce porosity [40] and reduce residual stresses [41]. Typically, an increase in mechanical properties by using certain hatch rotation angle is explained by the formation of a more uniform fine-grained structure. To study the effect of the hatch rotation angle on reducing the number of defects and increasing the plastic characteristics of the Ti-6Al-4V alloy, a series of SLM samples were manufactured to study the mechanical characteristics in the tensile mode. Fig. 7, *b* shows the dependence of the relative density of Ti-6Al-4V SLM samples on the hatch rotation angle. The minimum relative density of 99.3% was obtained on samples in which the hatching did not rotate relative to the previous layer (angle 0°). In this case, the scanning tracks are located directly above one another, which deteriorates the quality of the surface of the layer for melting, negatively affects the uniformity of the powder layer, and, ultimately, leads to the appearance of discontinuities and pores. The maximum relative density value of 99.8% was obtained on samples, the construction of which used the angle of hatch rotation relative to the previous layer 72°. Fig. 6, *d* shows an image of the area at the boundary between contours and hatching (the angle of hatch rotation relative to the previous layer is 72°), in which no defects characteristic of modes without optimization of scanning tactics are observed (Fig. 6, *c*). The results of the study showed that the use hatch rotation angle of 72° made it possible to increase the elongation to failure to 11% while maintaining the average values of the tensile strength of 1300 MPa and the yield stress of 1250 MPa.

Analyzing the results of optimization of scanning tactics in order to increase density, it should be noted that the use of optimal cell sizes in the case of using the „chessboard" scanning tactics allows increasing the relative density values to 99.95%. However, this type of scanning tactic cannot be used for creating thin-walled products. A more universal scanning tactic that provides high density is rotating the hatching relative to the previous layer. Using the hatch rotation angle 72° to the previous layer makes it possible to significantly increase the plastic characteristics of Ti-6Al-4V SLM samples without reducing the strength characteristics of the material. The obtained value of elongation to failure of 11% corresponds to the requirements for titanium alloys of the Ti-6Al-4V system, designed for use in the production of implants and endoprostheses [20].

Conclusion

Studies of the physical and mechanical properties of titanium alloy Ti-6Al-4V, processed by SLM, and optimization of SLM parameters were carried out. The following results were obtained and the main conclusions were drawn:

1. Samples of titanium alloy Ti-6Al-4V were processed by SLM with high mechanical characteristics (tensile strength 1300 MPa, yield strength 1250 MPa), which are 30% higher than the reference values for this alloy manufactured by traditional technologies (rolling, forging).

2. The dependences of the physical and mechanical characteristics of the Ti-6Al-4V SLM alloy on the main parameters of the SLM, i.e. diagrams of strength and plastic properties and density have been constructed. The optimal SLM parameters were determined to ensure high mechanical characteristics of the Ti-6Al-4V alloy: laser power 95 ± 5 W and scanning speed I125 ± 25 mm/s.

3. The reason for the increase in the strength characteristics of the Ti-6Al-4V SLM alloy may be the presence of a finely dispersed martensitic structure, which arises as a result of the high crystallization rates realized during SLM.

4. Optimization of the scanning tactics of SLM made it possible to increase the characteristics of the Ti-6Al-4V SLM alloy: the maximum value of the relative density increased to 99.8%, the elongation to failure was 11%, which meets the requirements for the Ti-6Al-4V alloy for use in surgery and endoprosthetics.

Funding

This study was financially supported by the grant of Russian Science Foundation 22-19-00271.

Conflict of interest

The authors declare that they have no conflict of interest.

References

[1] F. Bartolomeu, M.M. Costa, J.R. Gomes, N. Alves, C.S. Abreu, F.S. Silva, G. Miranda. Tribol. Int., **129**, 272 (2019). DOI: 10.1016/j.triboint.2018.08.012

[2] R. Krishna. *Titanium Alloys — Recent Progress in Design, Processing, Characterization, and Applications* (IntechOpen, 2023)

[3] C. Jaiswal. *Titanium Alloys Market Research Report Information By Type (commercially Pure Titanium, Titanium Alloys), By Application (Structural Airframes, Engines, Others), And By Region (North America, Europe, Asia-Pacific, And Rest Of The World)* — Market Forecast Till 2030 (USA, 2023)

[4] E. Fereiduni, A. Ghasemi, M. Elbestawi. Aerospace, **7** (6), 77 (2020). DOI: 10.3390/aerospace7060077

[5] N. Koju, S. Niraula, B. Fotovvati. Metals, **12**, 687 (2022). DOI: 10.3390/met12040687
[6] S. Rajendran, Mu. Naushad, D. Durgalakshmi, E. Lichtfouse (editors). *Metal, Metal Oxides and Metal Sulphides for Biomedical Applications* (Springer, NY., 2021)
[7] G. Lütjering, J.C. Williams. *Titanium Springer-Verlag* (Berlin, Heidelberg, 2003)
[8] R. Boyer, E.W. Collings, G. Welsch (editors). *Materials Properties Handbook: Titanium Alloys* (ASM International, 1994)
[9] M.Yu. Gryaznov, S.V. Shotin, V.N. Chuvildeev, A.N. Sysoev, N.V. Melekhin, A.V. Piskunov, N.V. Sakharov, A .V. Semenycheva, A.A. Murashov. ZhTF, **92** (2), 241 (2023). (in Russian). DOI: 10.21883/JTF.2023.02.54499.209-22
[10] Y. Bozkurt, E. Karayel. J. Mater. Res., **14**, 1430 (2021). DOI: 10.1016/j.jmrt.2021.07.050
[11] F. Liu, T. Zhou, T. Zhang, H. Xie, Y. Tang, P. Zhang. Mat. Des., **217**, 110630 (2022). DOI: 10.1016/j.matdes.2022.110630
[12] A.N. Aufa, M.Z. Hassan, Z. Ismail. J. Alloys Compd., **896**, 163072 (2022). DOI: 10.1016/j.jallcom.2021.163072
[13] Z. Guo, Ch. Wang, C. Du, J. Sui, J. Liu. Proc. CIRP, **89**, 126 (2020). DOI: 10.1016/j.procir.2019.12.003
[14] Z. Liang, X.Chen, Z.Sun, Y.Guo, Y. Li, H. Chang, L. Zhou. J. Manuf. Process, **84**, 414 (2022). DOI: 10.1016/j.jmapro.2022.09.041
[15] O.B. Perevalova, A.V. Panin, M.S. Kazachenok. ZhTF, **90** (3), 410 (2020). (in Russian). DOI: 10.21883/JTF.2020.03.48924.256-19
[16] J. Liu, Q. Sun, C. Zhou, X. Wang, H. Li, K. Guo, J. Sun. Mater. Sci. Eng. A, **766**, 138319 (2019). DOI: 10.1016/j.msea.2019.138319
[17] X.Yan, S. Yin, C. Chen, C. Huang, R. Bolot, R. Lupoi, M. Kuang, W. Ma, C. Coddet, H. Liao, M. Liu. J. Alloys Comp., **764**, 1056 (2018). DOI: 10.1016/j.jallcom.2018.06.076
[18] M. Shunmugavel, A. Polishetty, G. Littlefair. Proc. Technol., **20**, 231 (2015). DOI: 10.1016/j.protcy.2015.07.037
[19] E. Alabort, Y.T. Tang, D. Barba, R.C. Reed. Acta Mater., **229**, 117749 (2022). DOI: 10.1016/j.actamat.2022.117749
[20] GOST R ISO 5832-3:2021 *Implants for surgery. Metallic materials. Part 3. Wrought titanium 6-aluminium 4-vanadium alloy.* Official publication (International Standard published, 2021).
[21] P.A. Shweitzer. *Metallic Materials. Physical, Mechanical and Corrosion Properties* (Marcel Dekker, Inc. NY., USA, 2003)
[22] L.X. Meng, D.D. Ben, H.J. Yang, H.B. Ji, D.L. Lian, Y.K. Zhu, J. Chen, J.L. Yi, L. Wang, J.B. Yang, Z.F. Zhang. Mater. Sci. Eng. A, **815**, 141254 (2021). DOI: 10.1016/j.msea.2021.141254
[23] T. Rautio, A. Hamada, J. Mäkikangas, M. Jaskari, A. Järvenpää. Mater. Today: Proc., **28**, 907 (2020). DOI: 10.1016/j.matpr.2019.12.322
[24] P. Kumar, U. Ramamurty. Acta Mater., **194**, 305 (2020). DOI: 10.1016/j.actamat.2020.05.041
[25] S. Vaudreuil, S.-E. Bencaid, H.R. Vanaei, A. El Magri. Materials, **15**, 8640 (2022). DOI: 10.3390/ma15238640J
[26] Y. Yang, M. Zhao, H. Wang, K. Zhou, Y. He, Y. Mao, D. Xie, F. Lv, L. Shen. Appl. Sci., **13**, 1828 (2023). DOI: 10.3390/app13031828
[27] Y. Chen, S.J. Clark, C.L.A. Leung, L. Sinclair, S. Marussi, M.P. Olbinado, E. Boller, A. Rack, I. Todd, P.D. Lee. Appl. Mater. Today, **20**, 100650 (2020). DOI: 10.1016/j.apmt.2020.100650
[28] J. Liu, P. Wen. Mat. Des., 215, 110505 (2022). DOI: 10.1016/j.matdes.2022.110505
[29] L.-Ch. Zhang, H. Attar. Adv. Eng. Mater., **18** (4), 463 (2016). DOI: 10.1002/adem.201500419
[30] Z. Liang, Z. Sun, W. Zhang, S. Wu, H. Chang. J. Alloys Compd., **782** (25), 1041 (2019). DOI: 10.1016/j.jallcom.2018.12.051
[31] A.D. Baghi, S. Nafisi, R. Hashemi, H. Ebendorff-Heidepriem, R. Ghomashchi. J. Manuf. Process., **68**, 1031 (2021). DOI: 10.1016/j.jmapro.2021.06.035
[32] Y. Xiao, L. Lan, S. Gao, Bo He, Y. Rong. Mater. Sci. Eng. A, **858**, 144174 (2022). DOI: 10.1016/j.msea.2022.144174
[33] L. Zhou, T. Yuan, J.Z. Tang, J. He, R. Li. Opt. Laser Technol., **119**, 105625 (2019). DOI: 10.1016/j.optlastec.2019.105625
[34] Q. Yan, B. Chen, N. Kang, X. Lin, S. Lv, K. Kondoh, S. Li, J.S. Li. Mater. Charact., **164**, 110358 (2020). DOI: 10.1016/j.matchar.2020.110358
[35] Z.H. Jiao, R.D. Xu, H.C. Yu, X.R. Wu. Proc. Struct. Integr., **7**, 124 (2017). DOI: 10.1016/j.prostr.2017.11.069
[36] N. Rahulan, S.S. Sharma, N. Rakesh, R. Sambhu. Mater. Today: Proc., **56**, A7 (2022). DOI: 10.1016/j.matpr.2022.04.310
[37] *American Society for Testing Materials. ASTM FL108-14. Standard Specification for Titanium-6 Aluminum-4 Vanadium Alloy Castings for Surgical Implants* (UNS R56406) (ASTM International: West Conshohocken, PA, USA, 2014)
[38] S. Giganto, S. Martinez-Pellitero, J. Barreiro, P. Leo, M.A. Castro-Sastre. J. Mater. Res. Technol., **20**, 2734 (2022). DOI: 10.1016/j.jmrt.2022.08.040
[39] L.N. Carter, Ch. Martin, Ph.J. Withers, M.M. Attallah. J. Alloys Compd., **615**, 338 (2014). DOI: 10.1016/j.jallcom.2014.06.172
[40] T. Rautio, A. Mustakangas, J. Kumpula, A. Järvenpää. Proc. CIRP, **111**, 130 (2022). DOI: 10.1016/j.procir.2022.08.106
[41] J. Song, W. Wu, L. Zhang, B. He, L. Lu, X. Ni, Q. Long, G. Zhu. Optik, **170**, 342 (2018). DOI: 10.1016/j.ijleo.2018.05.128

Translated by V.Prokhorov